GEOPHYSICS, VOL. 77, NO. 5 (SEPTEMBER-OCTOBER 2012); P. E357–E363, 7 FIGS.
10.1190/GEO2011-0432.1

Quasi-analytical method for frequency-to-time conversion in CSEM applications

Ali Moradi Tehrani[1], Evert Slob[1], and Wim Mulder[2]

ABSTRACT

Frequency-to-time transformations are of interest to controlled-source electromagnetic methods when time-domain data are inverted for a subsurface resistivity model by numerical frequency-domain modeling at a selected, small number of frequencies whereas the data misfit is determined in the time domain. We propose an efficient, Prony-type method using frequency-domain diffusive-field basis functions for which the time-domain equivalents are known. Diffusive fields are characterized by an exponential part whose argument is proportional to the square root of frequency and a part that is polynomial in integer powers of the square root of frequency. Data at a limited number of frequencies suffice for the transformation back to the time. In the exponential part, several diffusion-time values must be chosen. Once a suitable range of diffusion-time values are found, the method is quite robust in the number of values used. The highest power in the polynomial part can be determined from the source and receiver type. When the frequency-domain data are accurately approximated by the basis functions, the time-domain result is also accurate. This method is accurate over a wider time range than other methods and has the correct late-time asymptotic behavior. The method works well for data computed for layered and 3D subsurface models.

INTRODUCTION

Controlled-source electromagnetic (CSEM) methods are generally divided into frequency-domain electromagnetic (FDEM) and time-domain (transient) electromagnetic (TDEM) methods, depending on the waveform of the transmitted electrical current. In the FDEM method, we measure the electromagnetic response caused by a time-periodic source current. The FDEM and TDEM fields are related by the Fourier transformation, and the TDEM field can thus be obtained as the Fourier transformation of FDEM data when recorded at a sufficient number of frequencies.

Modeling is a vital part of the interpretation in diffusive electromagnetic field data. For modeling in time, we can use fast frequency-domain modeling codes (Wannamaker et al., 1984; Alumbaugh et al., 1996; Abubakar and van den Berg, 2004; Zhdanov et al., 2006; Mulder et al., 2008; Tehrani and Slob, 2010) and then convert the results to the time domain with a suitable numerical method. An efficient transformation method will allow for the use of a limited number of important frequencies, thereby reducing the modeling effort during the inversion of time-domain data when the data fit is evaluated in the time domain (Druskin and Knizhnerman, 1994; Wirianto et al., 2011).

The Gaver-Stehfest method (Gaver, 1966; Stehfest, 1970) is one example of a numerical inverse Laplace transformation, but only works when the Laplace-domain data are available at machine (double) precision. Therefore, it is only applicable to solutions that are exactly known in the Laplace domain, but for which no closed-form expression exists in the time domain. There are several methods for computing time-domain electromagnetic data from frequency-domain data. One of these is the discrete Fourier transformation, which can be combined with cubic Hermite interpolation (Mulder et al., 2008). This leads to a transformation method requiring data at a limited number of optimally spaced frequencies, but the linear (equidistant) FFT usually requires over 10^5 points, which still is expensive if transients are needed at many receiver positions. The logarithmic FFT (Talman, 1978; Haines and Jones, 1988) is much faster, but reportedly less accurate than the linear FFT (Slob et al., 2010). The decay spectrum method (Newman et al., 1986) is another option. In this method, the time-domain EM signal is considered as a combination of several exponentially damped functions with unknown coefficients. The exponential damping factors are

Manuscript received by the Editor 27 October 2011; revised manuscript received 17 March 2012; published online 9 August 2012.
[1]Delft University of Technology, Department of Geoscience and Engineering, Delft, The Netherlands. E-mail: amoraditehrani@fugro-jason.com; e.c.slob@tudelft.nl.
[2]Delft University of Technology, Department of Geoscience and Engineering, Delft, The Netherlands; and Shell Global Solutions International BV, Rijswijk, The Netherlands. E-mail: wim.mulder@shell.com.

also unknown and must be chosen carefully. After solving for the coefficients in the frequency domain, the time-domain EM signal follows as a series of basis functions. The results of this Prony-type method are reported to be subjective and to require a lot of human interaction. Because the method expands the field in terms of damped exponentials, the late-time asymptote always has exponential decay.

None of the methods mentioned so far is considered suitable for accurate frequency-to-time transformation at a large number of receiver positions. We therefore continue with the method proposed in Slob and van den Berg (1999) and investigate if it works for arbitrary models, including the earth's surface and 3D models. We call it the "diffusion expansion method" (DEM). It uses the possibility to expand the electromagnetic field into a sequence of diffusive field basis functions with a known frequency dependence, but with unknown diffusion times that must be chosen based on the data to be transformed. It is therefore a Prony-type method, like the decay spectrum method, but with the advantage that the late-time behavior is always correct. The reason is that the expansion functions are diffusive-field time-functions, and therefore exhibit the time behavior of diffusive fields, whereas the decay spectrum method always creates fields with an exponential decay for late times. The diffusion expansion functions as a function of frequency have analytically known time-domain equivalents. Hence, once the expansion coefficients in the frequency domain have been found, the transient result is known by inspection for impulse, step, and ramp responses, whereas they can be obtained to machine precision by numerical integration for more complicated source time functions.

To obtain a quantitative measure, we first investigate how well the Gaver-Stehfest method (GSM), fast Fourier transformation (FFT), and the diffusion-expansion method (DEM) perform on problems where the time-domain solution is known exactly. We analyze how the choice of the range and number of diffusion-time values affect the results. We then compare the FFT method with DEM results for a three-layered medium and a 3D model, using numerical solutions. We find that DEM produces accurate results using only up to 30 frequency values and is robust in the choice of the number and range of diffusion-time values as long as the important values that characterize the data are incorporated in the range. The minimum value can be estimated from the high-frequency end of the data. It therefore seems a good candidate for accurate frequency-to-time transformation, and vice versa, requiring data values at only a limited number of frequencies.

THEORY

Numerical methods for frequency-domain to time-domain conversion

Modeling of the transient electromagnetic field for CSEM applications can be performed in an efficient way by first solving the problem in the frequency domain and then obtaining the time-domain solution by suitable numerical methods such as the decay spectrum method or the Fourier transformation. The Fourier transformation method is straightforward and fast if the number of frequencies can be kept small (Mulder et al., 2008; Slob et al., 2010). This method has been tested against exact solutions for some simple problems as well as a realistic marine example by Mulder et al. (2008). They showed that a limited number of frequencies suffices to provide time-domain solutions, employing piecewise-cubic Hermite interpolation to minimize the number of frequency points where data should be computed, followed by fast Fourier transformation of the data after interpolation to an equidistant (linear) frequency range. However, numerical results show that the time window where the obtained solution is accurate is limited and cannot be extended by incorporating more frequencies.

Quasi-analytical method for frequency-domain to time-domain conversion

Slob and van den Berg (1999) showed on scattered electromagnetic data from an object in a homogeneous embedding that the electric and magnetic fields can be expanded in diffusive decay functions as a sum of polynomials in $\sqrt{i\omega}$, each multiplied by functions that decay proportional to $\exp(-2\sqrt{i\omega\tau})$. Each power of $\sqrt{i\omega}$ has an unknown constant coefficient. The parameter τ is in principle unknown, but depends on the measurement configuration and the subsurface heterogeneity. The range of τ-values can span one or two decades, depending on the subsurface complexity and the time window of interest. The expansion functions used are canonical functions for the homogeneous space response to a point dipole excitation. The scattered field can always be expressed as an infinite sum of interactions of the scattering medium with the incident field that would exist in a homogeneous medium. For this reason, Slob and van den Berg (1999) argued that these functions can be used as expansion functions for the diffusive total electric and magnetic fields, but they only showed examples for a homogeneous 3D object embedded in a homogeneous space. Here we will show that the method is generally applicable, even in the presence of a nonconductive medium, which gives rise to functions that are different from the diffusion expansion functions. In the time domain, the airwave contributions to the electric and magnetic fields in the subsurface have late-time asymptotes that are inversely proportional to integer powers of time, whereas the other diffusive contributions all have late-time asymptotes inversely proportional to odd-integer powers of the square root of time (Slob et al., 2010). The airwave contributions are therefore represented in the frequency domain by different frequency-dependent functions than the diffusive fields that are not related to the airwave. Although the airwave related field is not properly accounted for, it can be approximated as a series of exponential diffusion functions. We therefore expect that the method will still perform well in the presence of a strong airwave related field and this is what we will show below.

The simplest way to implement this method is to determine a minimum and maximum value for τ and divide the time range up in $(k-1)$ equidistant time steps, $\tau_k = \tau_{\min} + (k-1)\Delta\tau$, $\tau_{\min}$ being the smallest diffusion time, and $\Delta\tau$ denoting the time step. Another straightforward way is to use an equidistant diffusion time step on a logarithmic axis. The maximum value of τ depends on the time window of interest, because the expansion functions are exponentially small for $\tau \gg t$. On the other hand, the smallest value of τ can be found from the slope of high-frequency logarithmic decay curve in the data. The smallest value of τ can always be estimated from the configuration if distance and conductivity are known.

The electric-field impulse response can be expanded as

$$\hat{E}^{\delta}(x^R, i\omega) \approx \sum_{k=1}^{K}\sum_{j=0}^{J} \alpha_{k,j}\hat{F}^{(j)}(\tau_k, i\omega), \qquad (1)$$

where $\hat{F}^{(j)}(\tau_k, i\omega) = (i\omega)^{j/2} \exp(-2\sqrt{i\omega\tau_k})$. The maximum power of $\sqrt{i\omega}$ depends on the type of source and can be taken as $J = 3$ for an electric current source and $J = 2$ for a magnetic current source. The higher frequencies become more important for higher values of J and in configurations where the high-frequency content is very small, $J = 2$ can also be chosen for an electric current source. The number of diffusion times, K, depends on the range of τ-values. Taking five to seven points per decade is usually sufficient. How to choose the range of τ-values is explained below. Because the coefficients $\alpha_{k,j}$ are strictly real, equation 1 is solved simultaneously for the real and imaginary parts of the electric field. For a step current source function, we should replace $\hat{F}^{(j)}(\tau, i\omega)$ by $\hat{F}^{(j-2)}(\tau, i\omega)$.

The time-domain equivalents of $\hat{F}^{(j)}(\tau, i\omega)$ are available in recursive form

$$F^{(j)}(\tau, t) = \frac{\sqrt{\tau}}{t} F^{(j-1)}(\tau, t) - \frac{j}{2t} F^{(j-2)}(\tau, t) \tag{2}$$

starting from the two functions

$$\begin{aligned} F^{(-2)}(\tau, t) &= \operatorname{erfc}(\sqrt{\tau/t}) H(t), \\ F^{(-1)}(\tau, t) &= \frac{\exp(-\tau/t)}{\sqrt{\pi t}} H(t), \end{aligned} \tag{3}$$

where "erfc" denotes the complementary error function. Functions for any other value of j can be obtained by combining equations 2 and 3. We have implemented the expansion given in equation 1 for the transformation back to time of the electric-field impulse response.

NUMERICAL RESULTS

All numerical examples were computed with double-precision arithmetic.

Half-space configurations

The first example is a VTI half-space below a nonconductive half-space. The source and receiver are located at the surface between the two half-spaces and their distance is given by $\mathbf{x}^R - \mathbf{x}^S = (2000, 0, 0)$ m. The horizontal and vertical conductivities are $\{\sigma^{(h)}, \sigma^{(v)}\} = \{0.1, 0.025\}$ S/m. The frequency- and time-domain responses are known in closed form for the x-component electric field generated by an x-component electric dipole source. We can therefore compare exact results with numerical results obtained with the GSM, the adaptive FFT, and the DEM. No specific modifications are needed to apply the DEM for an anisotropic medium because the anisotropy is accounted for by choosing the proper range of τ-values. The inline electric-field component measured on the surface generated by an x-directed electric current dipole is given by (Slob et al., 2010)

$$\begin{aligned} &E_{xx}(x^R - x^S, 0, 0) \\ &= \frac{1 - \exp(-2\sqrt{i\omega\tau_h}) + 2\sqrt{\sigma^{(h)}/\sigma^{(v)}}(1 + \sqrt{i\omega\tau_v}) \exp(-2\sqrt{i\omega\tau_v})}{2\pi\sigma^{(h)}(x^R - x^S)^3}, \end{aligned} \tag{4}$$

where $\tau_{h,v} = \sigma_{h,v}\mu_0(x^R - x^S)^2/4$ are the diffusion times corresponding to the horizontal and vertical conductivities, respectively. It can be seen from equation 4 that we can exactly model this field with the diffusion expansion method using three values for τ, being $\tau = 0$, $\tau = \tau_h$, and $\tau = \tau_v$. In the case of $\tau = 0$, we restrict J to zero because only a delta-pulse will be generated at $t = 0$ from this part. The highest power in $\sqrt{i\omega}$ in the polynomial part is unity, so we take $J = 1$ in that case.

For the adaptive FFT method, 39 frequencies, unevenly spaced on a logarithmic scale between 10^{-3} and 10^3 Hz, are necessary to retrieve accurate data at any other frequency by interpolation within the range and extrapolation for frequencies smaller than 1 mHz. The data are interpolated and extrapolated with 2^{21}, or about two million points, using a frequency interval $\Delta f \approx 2.38 \times 10^{-4}$ Hz, corresponding to a time step of $\Delta t = 0.1$ ms in the time domain. The same 39 frequencies are used in the DEM, with $K = 4$ and $J = 3$. To account for the impulse response that occurs in the data for a source and receiver located at the interface, we set $\tau_1 = 0$. For $k = 1$, we choose $J = 0$. Then $\tau_2 = 33$ ms, whereas $\tau_4 = 10\tau_2$ and $\tau_3 = (\tau_2 + \tau_4)/2$ is the midpoint between τ_2 and τ_4. The maximum normalized error in the DEM result is computed as the amplitude of the maximum difference, normalized by the amplitude of the data,

$$R^l_{\max} = \max\left(\frac{|E^{\mathrm{DEM}}(\omega) - E(\omega)|}{|E(\omega)|}\right) \tag{5}$$

and produces 1.2×10^{-5}. The normalized global rms error (RMSE) is the average error over all 39 frequencies used in the computation,

$$\mathrm{RMSE} = \sqrt{\frac{\sum_\omega |E^{\mathrm{DEM}}(\omega) - E(\omega)|^2}{\sum_\omega |E(\omega)|^2}} \tag{6}$$

and is 5.8×10^{-6}. From these frequency-domain results, we obtain time-domain results in a time window where the local normalized error is less than 5×10^{-2} given by $2.2 \times 10^{-3} \le t \le 100$ s and spans almost five decades. The results for all methods are displayed in Figure 1, where it can be seen that the FFT result suffers from numerical saturation, but the normalized error is less than 5×10^{-2} in the window $4 \times 10^{-3} \le t \le 1$ s, still spanning almost three decades. We observe also that the GSM produces very good results when the frequency-domain function is known explicitly.

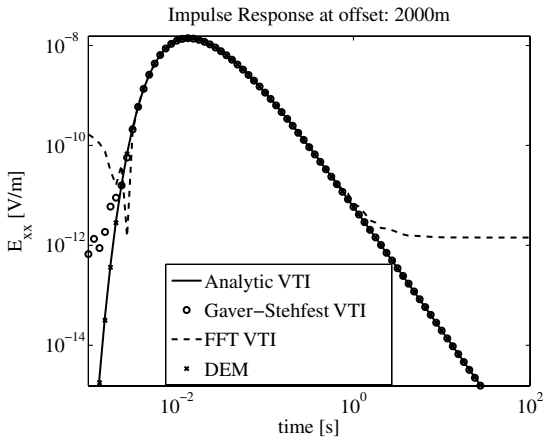

Figure 1. Electric-field impulse response for a source and receiver on the surface between a VTI half-space and a nonconductive half-space. The exact time-domain result is shown together with results from GSM, FFT, and DEM.

We can analyze the performance of DEM as a function of the choice and number of τ-values and the chosen maximum power of frequency. As written above, the exact representation is obtained with three diffusion-time values: $\tau_1 = 0$, $\tau_2 = \tau_v$, and $\tau_3 = \tau_h$; for τ_1, τ_2, $J = 0$, whereas for τ_3, $J = 1$. We will take $J = 0$ only for τ_0 and $J = 2$ for all other τ-values. We will vary K to see the effects on the obtained results. For this study, we use 13 frequency values sampled with a fixed spacing on a logarithmic axis from 10 mHz to 100 Hz and run DEM for different K-values with $\tau_1 = \tau_v/2$ and $\tau_K = 5\tau_h$. In this particular example with $J = 2$, the system is underdetermined for $K \geq 10$ because we have $(J+1)(K-1)+1$ unknown coefficients and 13 complex data points. We solve for the coefficients in the least-squares sense and keep the inversion stable by putting a small stabilizing number on the diagonal of the system matrix. The stabilizing number is taken as 10^{-12} times the trace of the system matrix. It can also be taken one or two orders of magnitudes smaller or bigger, modifying the results slightly, but also this number can be chosen over quite a large range without significantly changing the result. From these results, we conclude that if the frequency-domain data fit has errors at or below 10^{-5}, the time-domain results are accurate over a wide time range spanning four decades in time or more. Figure 2 shows the error in the obtained results for $J = 2$ and $K = 3, 6, 9, 12$. The time-domain results are computed from $t = 1$ ms to $t = 1000$ s and it can be seen

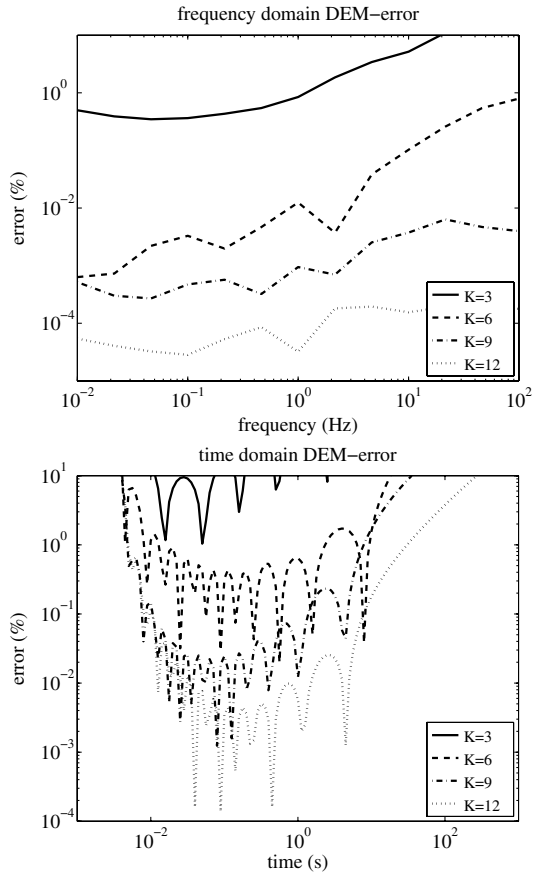

Figure 2. DEM data fit error in percentages in the frequency domain (top) and the corresponding error in the time-domain result (bottom), for $J = 2$ and a different number, but fixed range of τ-values from $\tau_2 = 15.7$ ms to $\tau_K = 314$ ms.

that for $K = 6$ the solution has an error less than 5% over a time range from 7 ms to 10 s.

The question of finding the smallest nonzero τ-value is answered by looking at the configuration and the high-frequency behavior of the electric field. The offset is known and source and receiver are located on the surface. The imaginary part of the electric field at high frequency is dominated by the term with the highest power in $\sqrt{i\omega}$ times the exponential containing the smallest nonzero τ-value. At these high frequencies, the ratio of the imaginary parts of the electric field at two distinct frequencies f_1 and f_2 can be written as

$$\frac{\mathrm{Im}\{E(f_2)\}}{\mathrm{Im}\{E(f_1)\}} \approx \frac{\cos\left(\sqrt{4\pi f_2 \tau_{\min}}\right) - \sin\left(\sqrt{4\pi f_2 \tau_{\min}}\right)}{\cos\left(\sqrt{4\pi f_1 \tau_{\min}}\right) - \sin\left(\sqrt{4\pi f_1 \tau_{\min}}\right)} \times \exp\left(-\sqrt{4\pi f_2 \tau_{\min}} + \sqrt{4\pi f_1 \tau_{\min}}\right), \quad (7)$$

from which $\tau_{\min}$ can be found by ignoring the ratio of the goniometric functions

$$\tau_{\min} \approx \frac{\log(\mathrm{Im}\{E(f_2)\}) - \log(\mathrm{Im}\{E(f_1)\})}{4\pi(f_1 + f_2) - 8\pi\sqrt{f_1 f_2}}. \quad (8)$$

Due to the goniometric functions, the result oscillates and we average over a small number of frequencies. In this example, we take data from 1 to 2 kHz in steps of 200 Hz to compute an average value for the minimum diffusion time of $\tau_{\min} \approx 0.024$, whereas the correct value is $\tau_v = \pi/100$. Obtaining an estimate that is too small is not detrimental to the result, as we have seen from the above results, whereas an overestimation does not allow the data to be accurately fitted by the model and gives a direct indication that $\tau_{\min}$ should be made smaller. Similarly, the maximum value for τ can easily be overestimated whereas underestimation may lead to inaccurate data fit.

Once accurate results have been found, it is easy to improve the results further by reducing the range of τ-values, and keeping the data fit in the frequency domain accurate. Figure 3 shows frequency data fit errors and resulting time-domain errors of DEM for the same range of K-values as shown in Figure 2, but in the τ-range with the estimated minimum value of $\tau_{\min} = 0.024$ s and $\tau_{\max} = 10\tau_{\min}$. It can be seen from the frequency-domain results in the top plot of Figure 3 that for $K = 3$ inaccurate results are obtained as the curve falls outside the plotted window. It can also be seen that the results for $K = 6$ are better at low frequencies than for $K = 9$, and that the results for $K = 6$ are more accurate at late times than the results for $K = 9$. The time-domain results are computed from $t = 1$ ms to $t = 1000$ s, and it can be seen that for $K = 6$ the solution has an error less than 5% over a time range from 3 ms to 900 s, increasing the time range by an order of magnitude compared to the initial τ-range used for inversion and these results are obtained with only 13 frequency values. Increasing the number of τ-values improves the results on the late-time side to well beyond 1000 s for $K = 12$.

Increasing both the conductivity values by an order of magnitude to $\{\sigma^{(h)}, \sigma^{(v)}\} = \{1, 0.25\}$ S/m and putting the source and receivers inside the VTI half-space will produce a strong airwave-related field because the source and receiver are below the surface with a horizontal offset much larger than their two-way vertical distance. We put the source at $\mathbf{x}^S = (0, 0, 75)$ m and the receiver at $\mathbf{x}^R = (2000, 0, 125)$ m. For the adaptive FFT method, 73

frequencies, unevenly spaced on a logarithmic scale between 10^{-3} Hz and 10^{3} Hz, are necessary to retrieve the data accurately by interpolation at any other frequency. Again, the data are interpolated or extrapolated with 2^{21} points using a frequency interval $\Delta f \approx 2.38 \times 10^{-4}$ Hz. We use 21 frequencies equally spaced on a logarithmic scale from 1 mHz and 1 kHz in the DEM, with $\tau_{\min} = 12.6$ ms and $\tau_{\max} = 11.4$ s, and we choose a logarithmic spacing to accommodate the large differences in diffusion times between the airwave related field and the direct field and set $K = 11$ and $J = 2$. The maximum normalized error in the DEM result is $R^{l}_{\max} = 10^{-4}$, up to $f = 125$ Hz, whereas it grows exponentially to $R^{l}_{\max} = 0.13$ at $f = 1$ kHz. The normalized global rms error RMSE $= 7 \times 10^{-7}$ over all 21 frequencies. For this example, the FFT-method requires 75 times more computational time than DEM. Reducing the FFT-length by a factor of four, the difference is reduced to a factor of 20. In this example, the field that must be transformed is known explicitly and it does not require much time to compute for many frequencies (only 2% of the total time for the FFT method), hence the difference in computation time is mostly caused by the difference between performing interpolation and FFT, and inverting the 33×33 matrix and computing the time functions using the inversion result. For a model that must be computed numerically, the difference between the two methods will be larger because the field should be known at more frequency values for interpolation and FFT than for DEM.

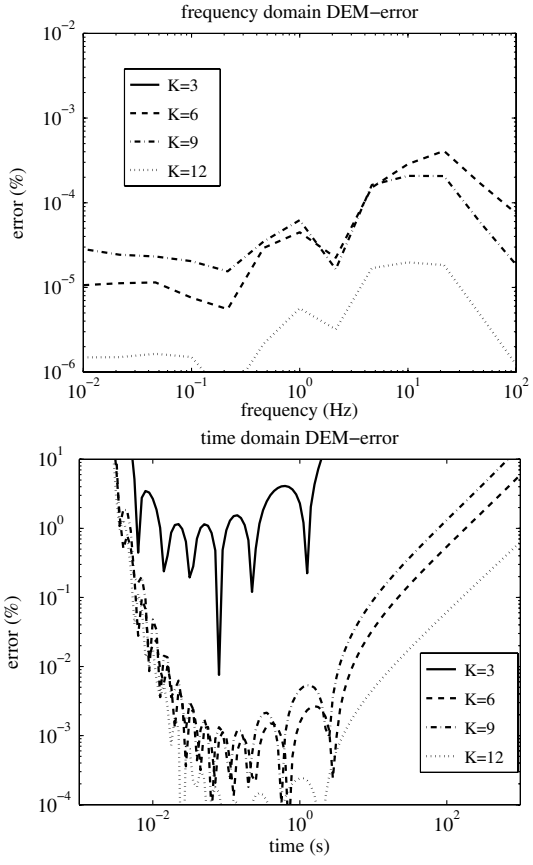

Figure 3. DEM data fit error in percentages in the frequency domain (top) and the corresponding error in the tim domain result (bottom), for $J = 2$ and a different number, but fixed range of τ-values from $\tau_2 = 24$ ms to $\tau_K = 240$ ms.

The local normalized error is less than 5×10^{-2} in the time window of $1 \times 10^{-3} \le t \le 1000$ s, spanning six decades, whereas it is less than 10^{-4} for $2 \times 10^{-3} < t < 10^{2}$ s, spanning almost five decades. Figure 4 shows the results for all methods. The FFT result suffers from numerical saturation, whereas the normalized error is less than 5×10^{-2} in the window $10^{-2} \le t \le 1$ s, spanning only two decades. This can be extended to earlier times by including higher frequencies, up 10 kHz, in the adaptive FFT, leading to computing the field at 85 frequency values and a time window where the local error is below the threshold of 5×10^{-2} down to 3 ms, whereas the upper limit is unchanged. We conclude that, for these simple VTI half-space examples, DEM produces very accurate time-domain data with a smaller number of frequency data points than necessary for FFT, over a much wider time range than the FFT method provides. The FFT method will work independently of the given subsurface geometry, whereas for DEM this remains to be demonstrated, which we will do next.

Three-layer configuration

We consider a three-layer example for which no explicit frequency-domain or time-domain solution exists. We make the step from known to unknown time-domain solutions and, based on what

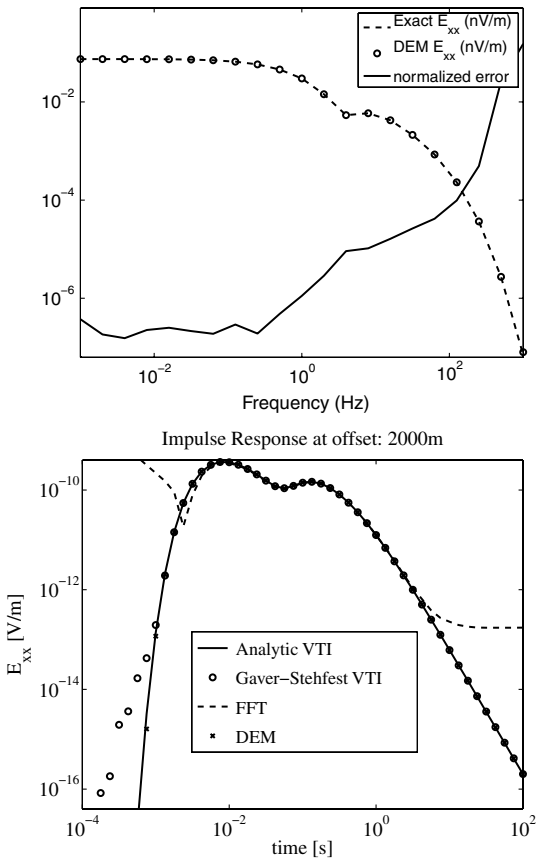

Figure 4. Electric-field impulse response for a source and receiver below the surface in the VTI half-space below a nonconductive half-space. The exact solution, data fit, and local normalized error are shown as a function of frequency (top) and the time-domain exact solution is shown together with results from GSM, FFT, and DEM (bottom).

was established in the above examples, we can assume that the late-time behavior is accurate. Therefore, we trust that the time-domain DEM results are accurate when the frequency-domain solution is fitted by the DEM with a small RMSE. Now, we apply the method to data obtained from modeling a three-layered earth configuration. The upper half-space is nonconductive, whereas the conductivity of the second layer and lower half-space are given by $\sigma_1 = 3$ S/m and $\sigma_2 = 1$ S/m, respectively. The second layer has a thickness of 1 km, an x-directed electric dipole source is placed 25 m above the bottom interface and the receiver measures the x-directed electric field at the bottom interface at 2-km offset in the x-direction, and at zero offset in the y-direction. We show the time-domain result of DEM and FFT in Figure 5. To obtain the DEM result, we used $K = 10$, $J = 2$ and a logarithmic spacing for τ between $\tau = 0.61$ s and $\tau = 311$ s. We used 33 frequencies logarithmically spaced between 1 mHz and 100 Hz. The global normalized error in the data fit was RMSE $= 6 \times 10^{-7}$. For FFT, the same frequency range was used and data at 113 frequency values were necessary for accurate interpolation. The same number of points were used for the linear FFT as described above. From this result, we see that adaptive FFT requires more than three times the number of data points for a result that is accurate over a much smaller time window than obtained with DEM.

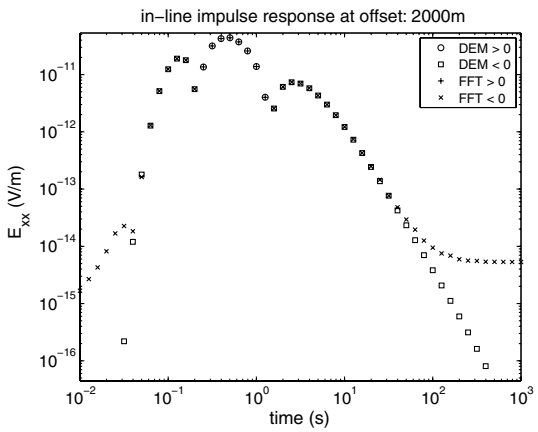

Figure 5. Time-domain results obtained with the DEM and the adaptive FFT for E_x, generated by J_x^e with 2 km offset in the x-direction in a three-layered earth configuration.

Three-layer model with a resistive 3D body

The three-layer model is modified to have shallower water and to include a 3D resistive body, mimicking a hydrocarbon reservoir as shown in Figure 6. The background conductivity in the lower half-space is 0.5 S/m, air has zero conductivity, and the sea water 3 S/m, whereas the resistive body has a conductivity of 0.02 S/m. The source is located 100 m above the sea bottom and a receiver is

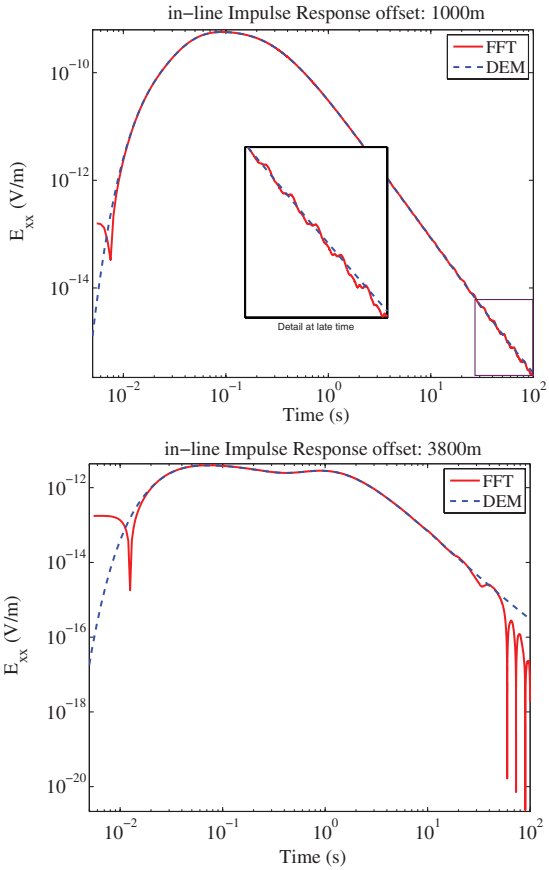

Figure 7. Electric field in 1000 m offset (top) and 3800 m offset (bottom) for a three-layer model with a 3D blocky reservoir. The optimized FFT result is marked by a solid line, and the DEM result by a dashed line.

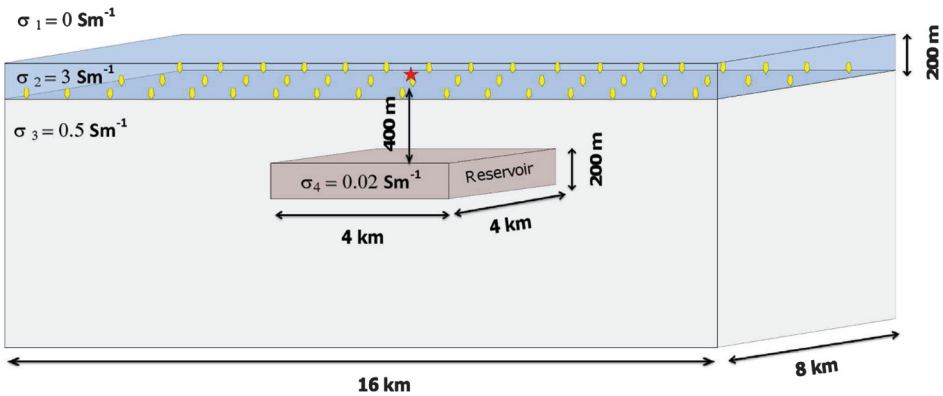

Figure 6. A three-layer earth model including an assumed reservoir.

placed on the sea bed. The water depth is 200 m. A resistive body has dimensions $4 \times 4 \times 0.2$ km^3, and its top is located at 400 m below the sea bed (Figure 4). The x-component of the electric field, generated by an x-directed electric dipole, is computed at an offset of 1 km as well as 3.8 km in the x-direction and at zero offset in the y-direction. Frequency-domain data in this 3D model were generated by a finite-volume code (Mulder, 2006). The FFT method produced a time-domain result using 61 frequencies, unequally spaced on a logarithmic axis, followed by cubic interpolation to a linear frequency axis using 10^6 points and a FFT, as described by Mulder et al. (2008).

For the DEM, we used 31 logarithmically spaced frequencies, ranging from 1 mHz to 1 kHz. We let $K = 10$ and $J = 2$, and set $\tau_{\min} = 0.135$ s and $\tau_{\max} = 25\tau_{\min}$. With these settings, we obtained a global RMSE of 1.8×10^{-4}. Figure 7 depicts the time-domain result for the DEM together with the result from the FFT. The two results agree very well in the time range from 20 ms to 8 s, but the FFT result at early time has a zero-crossing and even becomes negative before 8 ms, whereas it suffers from noise after 8 s and fluctuated in far offsets. The DEM solution is smooth and well-behaved over the whole plotted time range.

CONCLUSIONS

The diffusion expansion method is a good candidate for CSEM frequency-to-time conversion of data for any kind of subsurface model and survey configuration. The expansion contains the unknown expansion coefficients, multiplied by expansion functions whose time-domain equivalents are known. The latter consist of a polynomial term, with integer powers of the square root of frequency, as well as an exponential function whose argument is proportional to the square root of frequency. The proportionality factor contains a diffusion time that is unknown and must be estimated from the data. We have shown that this can be achieved by considering the high-frequency behavior of the data.

Because the frequency-domain expansion functions have analytically known time-domain equivalents, solving for the expansion coefficients is sufficient to obtain the transient field for different type for source time functions. If the electromagnetic field is generated by a step-response, the electromagnetic field that would have been generated by impulse or ramp source time functions can be obtained directly from the step response. Hence, it is straightforward to obtain the earth's impulse response from step-response data.

From the results obtained on functions that are known exactly in both the frequency and time domains, we found that the DEM produces accurate time-domain results when the frequency-domain fit is accurate. In the VTI half-space example with a strong airwave related signal, time-domain results were obtained with an error below 5% over a time window spanning almost six decades. Given the results obtained in the three-layer model and in the one with an additional 3D resistive body, we believe that accuracy of the frequency-domain data fit ensures an accurate time-domain result. In the examples, we found an error less than 5% in the time window spanning four decades.

The results obtained with the DEM appear to be more accurate over a wider time window than those obtained with a FFT, and the number of frequency values at which the frequency-domain data should be known is smaller, which means that modeling 3D data can be done at a smaller number of frequency values. The computation of each transient requires less time with the DEM than with the FFT, because for the FFT, typically in the order of 10^6 points, computed by cubic interpolation to an equally spaced frequency axis, should be used, whereas the DEM result is obtained after inverting a matrix of typical size 30×30, followed by multiplying the expansion coefficients with the transient expansion functions. The most time-consuming part can be to find the proper range of diffusion-time values that are input into the expansion functions. In our experience, this is not too difficult, but of course each human interaction requires time. Once a proper diffusion-time range is found for one receiver, it can be modified in an automated way for adjacent receivers. We found that the solution is quite robust for changes in the diffusion-time range.

ACKNOWLEDGMENTS

This research has been funded by the Delft Earth Research Center.

REFERENCES

Abubakar, A., and P. M. van den Berg, 2004, Iterative forward and inverse algorithms based on domain integral equation for three dimensional electric and magnetic objects: Journal of Computational Physics, **195**, 236–262, doi: 10.1016/j.jcp.2003.10.009.

Alumbaugh, D. L., G. A. Newman, L. Prevost, and J. N. Shadid, 1996, Three-dimensional wideband electromagnetic modeling on massively parallel computers: Radio Science, **31**, 1–23, doi: 10.1029/95RS02815.

Druskin, V. L., and L. A. Knizhnerman, 1994, Spectral approach to solving three-dimensional Maxwell's diffusion equations in the time and frequency domains: Radio Science, **29**, 937–953, doi: 10.1029/94RS00747.

Gaver, D. P., 1966, Observing stochastic processes and approximate transform inversion: Operations Research, **14**, 444–459, doi: 10.1287/opre.14.3.444.

Haines, G. V., and A. G. Jones, 1988, Logarithmic Fourier transformation: Geophysical Journal of the Royal Astronomical Society, **92**, 171–178, doi: 10.1111/gji.1988.92.issue-1.

Mulder, W. A., 2006, A multigrid solver for 3D electromagnetic diffusion: Geophysical Prospecting, **54**, 633–649, doi: 10.1111/j.1365-2478.2006.00558.x.

Mulder, W. A., M. Wirianto, and E. C. Slob, 2008, Time-domain modeling of electromagnetic diffusion with a frequency-domain code: Geophysics, **73**, no. 1, F1–F8, doi: 10.1190/1.2799093.

Newman, G., G. Hohmann, and W. Anderson, 1986, Transient electromagnetic response of a three-dimensional body in a layered earth: Geophysics, **51**, 1608–1672, doi: 10.1190/1.1442212.

Slob, E., J. Hunziker, and W. A. Mulder, 2010, Green's tensors for the diffusive electric field in a VTI half-space: Progress In Electromagnetics Research, **107**, 1–20, doi: 10.2528/PIER10052807.

Slob, E. C., and P. M. van den Berg, 1999, Integral-equation method for modeling transient diffusive electromagnetic fields: Three dimensional electromagnetics: SEG, 42–58.

Stehfest, H., 1970, Numerical inversion of Laplace transforms: Communications of the ACM, **13**, 47–49, doi: 10.1145/361953.361969.

Talman, J. D., 1978, Numerical Fourier and Bessel transforms in logarithmic variables: Journal of Computational Physics, **29**, 35–48, doi: 10.1016/0021-9991(78)90107-9.

Tehrani, A. M., and E. Slob, 2010, Fast and accurate three-dimensional controlled source electromagnetic modelling: Geophysical Prospecting, **58**, 1133–1146.

Wannamaker, P. E., G. W. Hohmann, and W. A. SanFilipo, 1984, Electromagnetic modeling of three-dimensional bodies in layered earths using integral equations: Geophysics, **49**, 60–74, doi: 10.1190/1.1441562.

Wirianto, M., R.-E. Plessix, and W. A. Mulder, 2011, Inversion of 3D time-domain electromagnetic data: The effect of time-weighting: 81st Annual International Meeting, SEG, Expanded Abstracts, 557–561.

Zhdanov, M. S., S. K. Lee, and K. Yoshioka, 2006, Integral equation method for 3D modeling of electromagnetic fields in complex structures with inhomogeneous background conductivity: Geophysics, **71**, no. 6, G333–G345, doi: 10.1190/1.2358403.